PHYSICAL REVIEW B **77**, 041407(R) (2008)

Pseudospin magnetism in graphene

Hongki Min,[1,*] Giovanni Borghi,[2] Marco Polini,[2] and A. H. MacDonald[1]
[1]*Department of Physics, The University of Texas at Austin, Austin, Texas 78712, USA*
[2]*NEST-CNR-INFM and Scuola Normale Superiore, I-56126 Pisa, Italy*
(Received 4 December 2007; published 17 January 2008)

We predict that neutral graphene bilayers are pseudospin magnets in which the charge density contribution from each valley and spin spontaneously shifts to one of the two layers. The band structure of this system is characterized by a momentum-space vortex, which is responsible for unusual competition between band and kinetic energies, leading to symmetry breaking in the vortex core. We discuss the possibility of realizing a pseudospin version of ferromagnetic metal spintronics in graphene bilayers based on hysteresis associated with this broken symmetry.

DOI: 10.1103/PhysRevB.77.041407 PACS number(s): 71.10.−w, 71.15.−m, 75.10.−b, 75.30.Kz

Introduction. The ground state of an interacting electron system flows from subtle compromises between band and interaction energy minimization. Because of the Pauli blocking effects that underlie Fermi liquid theory, however, the consequences of interactions are normally only quantitative[1] unless symmetries are broken. Recent progress[2] in the isolation of single and double sheets of carbon atoms (graphene sheets) has presented researchers with a new type of interacting electron system whose properties are now being actively explored,[3–5] both theoretically and experimentally. In this Rapid Communication we argue that band energy minimization is exceptionally frustrating to interactions in graphene bilayers, and predict that broken symmetry states in which charge shifts spontaneously from one layer to the other occur as a consequence.

Graphene bilayers with Bernal stacking have one low-energy site per unit cell in each layer. When the layer degree of freedom is described as a pseudospin, the continuum limit of the π-orbital band Hamiltonian corresponds[6,7] to a pseudospin field $\boldsymbol{B}_{\rm band}=[\hbar^2k^2/(2m^\star)]\ (\cos(2\phi_{\boldsymbol{k}}),\sin(2\phi_{\boldsymbol{k}}),0)$, where $\phi_{\boldsymbol{k}}=\arctan(k_y/k_x)$, $m^\star=\gamma_1/(2v_{\rm F}^2)$, γ_1 is the interlayer tunneling amplitude, and $v_{\rm F}$ is the electron velocity at the Fermi energy in an isolated neutral graphene sheet. When interactions are neglected, the ground state of a neutral bilayer has a full valence band of pseudospinors aligned at each $\boldsymbol{k}$ with this pseudospin field, forming the momentum-space vortex. The vortex exacts a large interaction energy penalty because of its rapid pseudospin-orientation variation. We propose that, like its real-space counterpart,[8] the momentum-space vortex sidesteps this energy cost by forming a vortex core in which the pseudospin orientation is out of plane in either the $\hat{z}$ or $-\hat{z}$ direction, as illustrated in Fig. 1. The momentum-space vortex state is nonuniform in momentum space, but in real space transfers charge uniformly between layers. Our paper starts by describing a technical calculation that supports and elaborates on our prediction and then discusses anticipated properties of this state.

Chiral two-dimensional electron system Hartree-Fock theory. It is instructive to consider a class of chiral two-dimensional electron system (C2DES) models which includes the continuum limits of single-layer and bilayer graphene sheets as special cases. These C2DES models have band Hamiltonians

$$\hat{\mathcal{H}}_{\rm band}=-\sum_{\boldsymbol{k},\sigma',\sigma}\hat{c}^\dagger_{\boldsymbol{k},\sigma'}\left[\varepsilon_0(k_{\rm c})\left(\frac{k}{k_{\rm c}}\right)^J[\cos(J\phi_{\boldsymbol{k}})\tau^x_{\sigma',\sigma}+\sin(J\phi_{\boldsymbol{k}})\tau^y_{\sigma',\sigma}]+\frac{V_{\rm g}}{2}\tau^z_{\sigma',\sigma}\right]\hat{c}_{\boldsymbol{k},\sigma},\qquad(1)$$

where σ, σ' are pseudospin labels, J is the chirality index, τ^a is a Pauli matrix, $k_{\rm c}$ is the model's ultraviolet momentum cutoff, $\varepsilon_0(k_{\rm c})$ is the energy scale of the band Hamiltonian, and a sum over valley and spin components is implicit. In Eq. (1), $V_{\rm g}$ is an external potential term that couples to the pseudospin magnet order parameter and corresponds in the case of bilayer graphene to an external potential difference between the layers. For single-layer graphene $J=1$ and $\varepsilon_0(k_{\rm c})=\hbar v_{\rm F}k_{\rm c}$, while for bilayer graphene $J=2$ and $\varepsilon_0(k_{\rm c})$

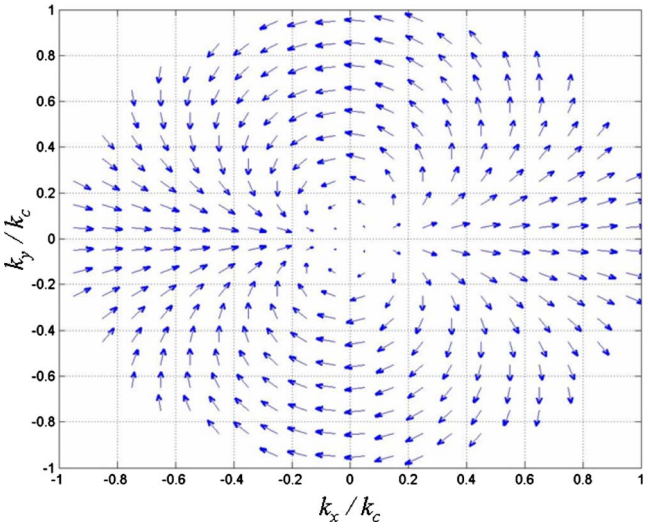

FIG. 1. (Color online) Pseudospin orientation in a graphene bilayer broken symmetry state. In this figure the arrows represent both the magnitude and the direction of the $\hat{x}$-$\hat{y}$ projection of the pseudospin orientation $\hat{n}$ as obtained from a mean-field-theory calculation for a neutral, unbiased bilayer with coupling constant $\alpha=1$. The arrows are shorter in the core of the momentum-space vortex because the pseudospins in the core have rotated spontaneously toward the $\hat{z}$ or $-\hat{z}$ direction.

$=\hbar^2 k_c^2/(2m^\star)$. The dimensionless coupling constant of these C2DESs, which measures the interaction strength, can be defined as $\alpha=(e^2k_c/\epsilon)/\varepsilon_0(k_c)$ where ϵ is the effective dielectric function due to screening external to the π-electron system. In the case of a single graphene layer $\alpha_{\rm mono}=e^2/(\epsilon v_F\hbar)$, while in the bilayer case, $\alpha_{\rm bi}=2e^2/(\epsilon v_c\hbar)$, where $v_c=\hbar k_c/m^\star$. If we choose[9] $\hbar k_c=\sqrt{2m^\star\gamma_1}$ for the bilayers, we have $\alpha_{\rm bi}=\alpha_{\rm mono}$. Typically $\epsilon\sim 2.5$, which implies a dimensionless coupling constant $\alpha\sim 1$. We use $\varepsilon_0(k_c)$ and k_c^{-1} as energy and length units in the rest of this paper.

The C2DES Hartree-Fock Hamiltonian can be written (in dimensionless units) in the following physically transparent form:

$$\hat{\mathcal{H}}_{\rm HF}=-\sum_{\boldsymbol{k},i,\sigma',\sigma}\hat{c}^\dagger_{\boldsymbol{k},i,\sigma'}\mathcal{B}^{(i)}_{\sigma',\sigma}(\boldsymbol{k})\hat{c}_{\boldsymbol{k},i,\sigma}, \tag{2}$$

where $\mathcal{B}^{(i)}_{\sigma',\sigma}=B^{(i)}_0(\boldsymbol{k})\delta_{\sigma',\sigma}+\boldsymbol{B}^{(i)}(\boldsymbol{k})\cdot\boldsymbol{\tau}_{\sigma',\sigma}$,

$$B^{(i)}_0(\boldsymbol{k})=\alpha\int_{|\boldsymbol{k}'|<1}\frac{d^2\boldsymbol{k}'}{2\pi}\frac{1}{|\boldsymbol{k}-\boldsymbol{k}'|}\frac{f^{(i)}_{\rm sum}(\boldsymbol{k}')}{2}, \tag{3}$$

and the pseudospin field $\boldsymbol{B}^{(i)}(\boldsymbol{k})$ has band and interaction contributions

$$B^{(i)}_x(\boldsymbol{k})=k^J\cos(J\phi_{\boldsymbol{k}})+\alpha\int_{|\boldsymbol{k}'|<1}\frac{d^2\boldsymbol{k}'}{2\pi}\frac{e^{-|\boldsymbol{k}-\boldsymbol{k}'|\bar{d}}}{|\boldsymbol{k}-\boldsymbol{k}'|}\frac{f^{(i)}_{\rm diff}(\boldsymbol{k}')}{2}n^{(i)}_x(\boldsymbol{k}'), \tag{4}$$

$$B^{(i)}_y(\boldsymbol{k})=k^J\sin(J\phi_{\boldsymbol{k}})+\alpha\int_{|\boldsymbol{k}'|<1}\frac{d^2\boldsymbol{k}'}{2\pi}\frac{e^{-|\boldsymbol{k}-\boldsymbol{k}'|\bar{d}}}{|\boldsymbol{k}-\boldsymbol{k}'|}\frac{f^{(i)}_{\rm diff}(\boldsymbol{k}')}{2}n^{(i)}_y(\boldsymbol{k}'), \tag{5}$$

$$B^{(i)}_z(\boldsymbol{k})=\frac{\bar{V}_g}{2}+\alpha\sum_j\int_{|\boldsymbol{k}'|<1}\frac{d^2\boldsymbol{k}'}{2\pi}\left(\frac{1}{|\boldsymbol{k}-\boldsymbol{k}'|}\delta_{i,j}-\bar{d}\right)\times\frac{f^{(j)}_{\rm diff}(\boldsymbol{k}')}{2}n^{(j)}_z(\boldsymbol{k}'). \tag{6}$$

Here i, j label the four valley and spin components of graphene's $J=1$ and $J=2$ C2DESs, $\boldsymbol{n}^{(i)}(\boldsymbol{k})$ is the direction of $\boldsymbol{B}^{(i)}(\boldsymbol{k})$, $f^{(i)}_{\rm sum}(\boldsymbol{k}')$ $[f^{(i)}_{\rm diff}(\boldsymbol{k}')]$ is the sum of (difference between) low- and high-energy occupation numbers, $\bar{V}_g=V_g/\varepsilon_0(k_c)$ is the gate potential in units of $\varepsilon_0(k_c)$, $\bar{d}=k_cd$ is the distance between layers in units of k_c^{-1} in the bilayer case, and $\bar{d}=0$ in the monolayer case. The term proportional to $\bar{d}$ on the right-hand side of Eq. (6) is the Hartree potential, which opposes charge transfer between layers in the bilayer case.

Local minima of the Hartree-Fock energy functional solve Eqs. (4)–(6) self-consistently. Our focus here is on the broken symmetry momentum-space vortex solutions in which pseudospins near $\boldsymbol{k}=\boldsymbol{0}$ tilt away from their band Hamiltonian $\hat{x}$-$\hat{y}$ plane orientations toward the $\pm\hat{z}$ direction, i.e.,

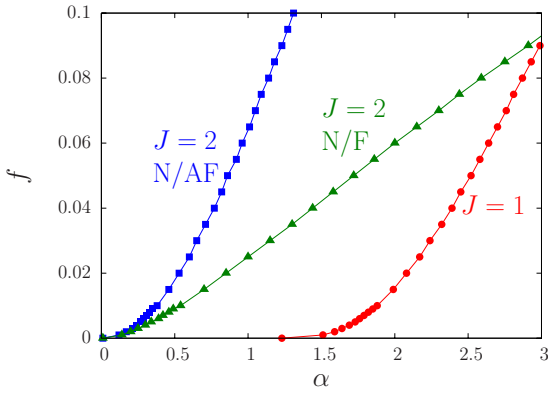

FIG. 2. (Color online) Phase diagrams of C2DESs with $J=2$ and 1. For the $J=2$ bilayer case we have taken $\bar{d}=0.2$. Pseudospin magnetism occurs at strong coupling α and weak doping f. $(1+f=n_\uparrow+n_\downarrow$ where the pseudospin density $n_\sigma=\Sigma_{\boldsymbol{k},i}\langle\hat{c}^\dagger_{\boldsymbol{k},i,\sigma}\hat{c}_{\boldsymbol{k},i,\sigma}\rangle/\mathcal{N}$ and $\mathcal{N}=\Sigma_{\boldsymbol{k},i}1.)$ In the $J=2$ bilayer case, the Hartree potential favors smaller total polarization so that the initial normal (N) state instability (blue separatrix) is to antiferromagnetic (AF) states in which the pseudospin polarizations of different valley and spin components cancel. At larger α, the normal state is unstable (green separatrix) to ferromagnetic (F) pseudospin states. In the $J=1$ monolayer case $\bar{d}=0$ so the phase boundaries (red separatrix) of F and AF broken-symmetry states coincide.

$$\boldsymbol{n}^{(i)}(\boldsymbol{k})=(n^{(i)}_\perp(k)\cos(J\phi_{\boldsymbol{k}}),n^{(i)}_\perp(k)\sin(J\phi_{\boldsymbol{k}}),n^{(i)}_z(k))$$

with $[n^{(i)}_\perp(k)]^2+[n^{(i)}_z(k)]^2=1$. Pseudospin polarization in the $\hat{z}$ direction corresponds to charge transfer between layers. This ansatz yields effective magnetic fields whose $\hat{x}$-$\hat{y}$ plane projections are parallel to the band Hamiltonian effective field. We find that $\boldsymbol{B}^{(i)}(\boldsymbol{k})=(B^{(i)}_\perp(k)\cos(J\phi_{\boldsymbol{k}}),B^{(i)}_\perp(k)\sin(J\phi_{\boldsymbol{k}}),B^{(i)}_z\times(k))$ with

$$B^{(i)}_\perp(k)=k^J+\alpha\int_0^1 dk'F_\perp(k,k')f^{(i)}_{\rm diff}(k')n^{(i)}_\perp(k'), \tag{7}$$

$$B^{(i)}_z(k)=\frac{\bar{V}_g}{2}+\alpha\sum_j\int_0^1 dk'\left(F_z(k,k')\delta_{i,j}-\frac{1}{2}k'\bar{d}\right)\times f^{(j)}_{\rm diff}(k')n^{(j)}_z(k'), \tag{8}$$

where the exchange kernels in Eqs. (7) and (8) are given by

$$F_\perp(k,k')=k'\int_0^\pi\frac{d\phi}{2\pi}\frac{e^{-q\bar{d}}}{q}\cos(J\phi),$$

$$F_z(k,k')=k'\int_0^\pi\frac{d\phi}{2\pi}\frac{1}{q}, \tag{9}$$

with $q=q(k,k',\phi)\equiv\sqrt{k^2+k'^2-2kk'\cos(\phi)}$. The pseudospin-chirality-induced frustration is represented by the factor $\cos(J\phi)$ in the first line of Eq. (9) which makes $F_\perp$ much smaller than F_z.

Pseudospin magnet phase diagram. We test the stability of the "normal" state $[n^{(i)}_z(k)\equiv 0$ at $V_g=0]$ solution of the

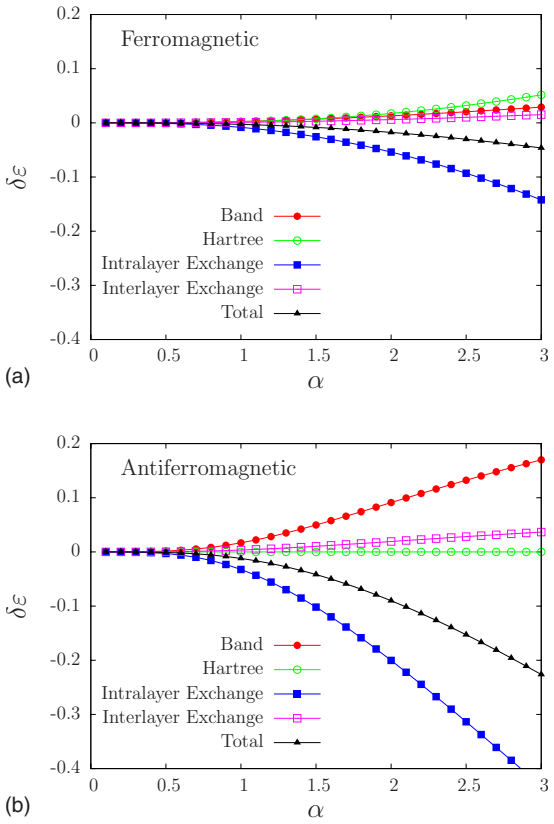

FIG. 3. (Color online) Condensation energy per electron $\delta\varepsilon$ [in units of $\varepsilon_0(k_c)$] as a function of α for an undoped ($f=0$) $J=2$ C2DES. This figure shows results for both F (top) and AF (bottom) states.

Hartree-Fock equations by linearizing the self-consistency condition; $n_z^{(i)} = B_z^{(i)} n_\perp^{(i)} / B_\perp^{(i)} \to B_z^{(i)} / B_\perp^{(i)}|_{n_z^{(i)}\equiv 0}$. This gives a k-space integral equation

$$n_z^{(i)}(k) = \sum_j \int_0^1 dk' M_{i,j}(k,k') n_z^{(j)}(k'), \tag{10}$$

where

$$M_{i,j}(k,k') = \frac{\alpha[F_z(k,k')\delta_{i,j} - k'\bar{d}/2] f_{\rm diff}^{(j)}(k')}{k^J + \alpha \int_0^1 dk'' F_\perp(k,k'') f_{\rm diff}^{(i)}(k'')}. \tag{11}$$

The normal state is stable when the largest eigenvalue of the linear integral operator $\mathcal{M}$ in the right-hand side of Eq. (10) is smaller than 1. Eigenvalues larger than 1 are possible only because $F_\perp$ is smaller than F_z, i.e., because of pseudospin chirality. Phase diagrams for $J=2$ and 1 are plotted in Fig. 2. The pseudospin magnet is more stable for larger coupling constant because it is driven by interactions, for larger J because the typical value of the band energy term, proportional to k^J, decreases with J, and for smaller doping because $f_{\rm diff}^{(i)}(k)$ is then nonzero in a larger region of k space. The eigenvectors of $\mathcal{M}$ specify the instability channel. The component-index structure of $\mathcal{M}$ implies that the eigenvalues occur in groups of four, three of which [labeled *antiferromagnetic* (AF) in Fig. 2] correspond in bilayers to states with no net charge transfer, i.e., $\Sigma_j n_z^{(j)}(k) \equiv 0$. The *ferromagnetic* (F) instability in which all components are polarized in the same sense is opposed by the Hartree potential and delayed to larger coupling constant. For both AF and F instabilities, $n_z(k)$ is peaked at small k where the $\hat{x}$-$\hat{y}$ pseudospin-plane exchange energies are most strongly frustrated by chirality, and the kinetic energy term which opposes pseudospin magnetism is weakest.

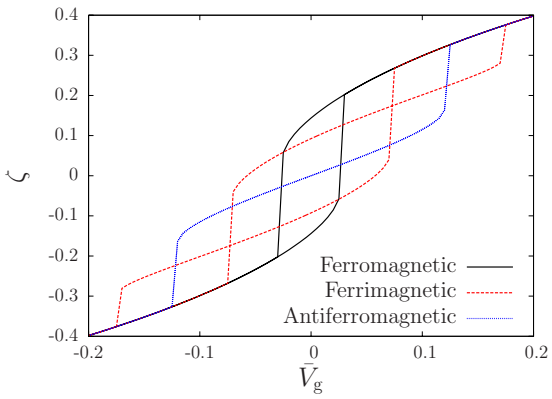

FIG. 4. (Color online) Metastable configurations of the pseudospin ferromagnet as a function of bias voltage V_g [in units of $\varepsilon_0(k_c)$] with $\alpha=1$ and $f=0$. We find self-consistent solutions of the gap equations (7) and (8) in which the pseudospin polarization has the same sense in all four components (ferromagnetic), in three of the four components (ferrimagnetic), or in half of the four components (antiferromagnetic).

The physics that drives pseudospin magnetism in graphene bilayers is illustrated in Fig. 3, which partitions the condensation energy into band, Hartree, intralayer exchange, and interlayer exchange contributions. Spontaneous layer polarization lowers the intralayer interaction energy at a cost in all other components. The overall energy change is negative, and the broken symmetry state occurs, because the interlayer exchange energy of the normal state is weakened by the band-Hamiltonian-induced frustration explained earlier. The cost in interlayer exchange energy of pseudospin rotation is therefore much smaller than the gain in intralayer exchange energy and the overall energy is reduced. The energy gain is considerably larger for AF broken symmetry states.

Pseudospintronics. In Fig. 4 we illustrate typical results for the pseudospin (layer) polarization $\zeta=(n_\uparrow - n_\downarrow)/(n_\uparrow + n_\downarrow)$ of a graphene bilayer as a function of gate voltage $\bar{V}_g$. The AF ground state at $\bar{V}_g=0$, which has $[Z_2 \times SU(4)]/[SU(2) \times SU(2)]$ broken symmetry because of the freedom to choose any two spin or pseudospin components for (say) positive polarization, is gradually polarized by the gate voltage, but eventually becomes unstable in favor of polarizing more layers in the sense preferred by the gate voltage. At sufficiently strong gate voltages, the F ground state in which all layers are polarized in the same sense becomes the ground state. As the gate voltage is varied local minima of the Hartree-Fock energy functional become saddle points which are in the basin of attraction of another local minima. In this way, the self-consistent solutions exhibit hysteretic behavior.

If only the fully polarized solutions existed these results for pseudospin polarization as a function of gate voltage would be very much like the behavior expected for an easy-axis ferromagnet in an external magnetic field along the hard axis. In magnetic memories bistability enables information storage. In magnetic metal spintronics the dependence of the resistance of a circuit containing magnetic elements on the magnetization orientation of those elements gives rise to sudden changes in resistance with field (giant magnetoresistance) which can be used to sense very small magnetic fields. Currents running through such a circuit can also be used to change the magnetic state through spin-transfer torques. Pseudospin ferromagnetism in graphene bilayers could potentially lead to very appealing electrical analogs of both of these effects. Because of the collective behavior of many electrons, the pseudospin ferromagnet can be switched between metastable states with gate voltages that are much smaller than the thermal energy k_BT, potentially enabling electronics which is very similar to a standard complementary metal-oxide-semiconductor but uses much less power. This possibility is analogous to the property that a magnetic element can be switched between magnetic states by Zeeman field changes that are extremely small compared to the thermal energy k_BT. Pseudospin-transfer torques, which are expected to occur in electronic bilayer systems,[10] can also be used to switch the pseudomagnetic state.

Discussion. The proposals made here are based on approximate calculations and must ultimately be confirmed by experiment. Indeed, it is well known that Hartree-Fock theory (HFT) often overestimates the tendency toward broken symmetry states. For example HFT predicts that a nonchiral 2DES is a (real-spin) ferromagnet at moderate coupling strengths, whereas experiments and accurate quantum Monte Carlo calculations suggest that ferromagnetism occurs only at a quite large value of the coupling constant.[1] Nilsson *et al.*[11] have recently claimed that a similar ferromagnetic instability occurs in weakly doped graphene bilayers, presumably only at a much stronger coupling constant than implied by HFT. We believe that the momentum-space vortex instability identified here, which is unique to the peculiar band structure of bilayer graphene, is qualitatively more robust than the real-spin ferromagnetic instability. This should be especially true in neutral bilayers since the momentum-space vortex instability occurs at a coupling constant $(\alpha \to 0)$ for which correlation corrections to HFT are weak. This is not a strong-coupling instability like ferromagnetism, but much more akin to the very robust attractive-interaction weak-coupling instability which leads to superconductivity. The condensation energy per electron associated with the formation of a momentum-space vortex core is $\sim e^2 k_c/\epsilon$, much larger than the $\sim e^2 k_F/\epsilon$ condensation energy for the spin-polarized state. Because this broken symmetry state is most robust for uniform neutral bilayers, the smooth but strong disorder potentials responsible for inhomogeneity[12] in nearly neutral graphene sheets may need to be limited to allow this physics to emerge.

Work at UT Austin was supported by the Welch Foundation, NRI-SWAN, ARO, and DOE.

*hongki@physics.utexas.edu

[1] G. F. Giuliani and G. Vignale, *Quantum Theory of the Electron Liquid* (Cambridge University Press, Cambridge, U.K., 2005).

[2] K. S. Novoselov, A. K. Geim, S. V. Morozov, D. Jiang, Y. Zhang, S. V. Dubonos, I. V. Grigorieva, and A. A. Firsov, Science **306**, 666 (2004).

[3] K. S. Novoselov, A. K. Geim, S. V. Morozov, D. Jiang, M. I. Katsnelson, I. V. Grigorieva, S. V. Dubonos, and A. A. Firsov, Nature (London) **438**, 197 (2005).

[4] Y. Zhang, Y.-W. Tan, H. L. Stormer, and P. Kim, Nature (London) **438**, 201 (2005).

[5] For recent technical and popular reviews see A. K. Geim and K. S. Novoselov, Nat. Mater. **6**, 183 (2007); A. K. Geim and A. H. MacDonald, Phys. Today **60** (8), 35 (2007).

[6] K. S. Novoselov, E. McCann, S. V. Morozov, V. I. Fal'ko, M. I. Katsnelson, U. Zeitler, D. Jiang, F. Schedin, and A. K. Geim, Nat. Phys. **2**, 177 (2006).

[7] E. McCann and V. I. Fal'ko, Phys. Rev. Lett. **96**, 086805 (2006).

[8] See, for example, V. S. Pribiag, I. N. Krivorotov, G. D. Fuchs, P. M. Braganca, O. Ozatay, J. C. Sankey, D. C. Ralph, and R. A. Buhrman, Nat. Phys. **3**, 498 (2007), and work cited therein.

[9] H. Min, B. Sahu, S. K. Banerjee, and A. H. MacDonald, Phys. Rev. B **75**, 155115 (2007).

[10] S. H. Abedinpour, Marco Polini, A. H. MacDonald, B. Tanatar, M. P. Tosi, and G. Vignale, Phys. Rev. Lett. **99**, 206802 (2007).

[11] J. Nilsson, A. H. Castro Neto, N. M. R. Peres, and F. Guinea, Phys. Rev. B **73**, 214418 (2006).

[12] J. Martin, N. Akerman, G. Ulbricht, T. Lohmann,J. H. Smet, K. von Klitzing, and A. Yacoby, Nat. Phys., doi:10.1038/nphys781 (2007).